



# Rotary resonance echo double resonance for measuring heteronuclear dipolar coupling under MAS

Zhehong Gan \*

*Center of Interdisciplinary Magnetic Resonance, National High Magnetic Field Laboratory, Tallahassee, FL 32310, USA*

Received 16 June 2006; revised 17 August 2006

## Abstract

A rotary resonance echo double resonance (R-REDOR) experiment is described for measuring heteronuclear dipolar coupling under magic-angle spinning. Rotary resonance reintroduces both dipolar coupling and chemical shift anisotropy with an rf field matching the spinning frequency. The resonance effect from chemical shift anisotropy can be refocused with a rotary resonance echo. The R-REDOR experiment thus measures the dephasing of the rotary resonance echo from the heteronuclear dipolar coupling to determine the dipolar coupling constant. The rotary resonance experiment is suitable for measuring dipolar coupling with quadrupolar nuclei because it applies the recoupling rf only to the observed spin-1/2. The rotary resonance scheme has the advantages of a long  $T_2'$  and susceptible to spinning frequency fluctuation.

© 2006 Published by Elsevier Inc.

*Keywords:* Rotary resonance; R-REDOR; REDOR; MAS; Dipolar coupling

## 1. Introduction

Rotational echo double resonance (REDOR) experiment is a popular method for measuring heteronuclear distances in solids. The experiment applies a train of rotor-synchronized  $\pi$ -pulses under magic-angle spinning (MAS) to reintroduce the dipolar coupling and it measures the dephasing of rotational echo for determining the coupling constant [1,2]. An attractive feature of this experiment is that the dipolar dephasing can be fit with a universal REDOR curve depending only on the dipolar coupling constant. The simplicity and robustness of the experiment make REDOR a widely used method for distance measurement in solids [3–7].

The pulse sequences of REDOR and its variations can be divided into three types [8–13]. The first type is the most popular one. It applies a train of evenly spaced  $\pi$ -pulses (two per rotor cycle) to the coupled spin and one  $\pi$ -pulse

in the middle to the observed spin. The second type applies a train of  $\pi$ -pulse with one per rotor cycle to both spins with their timing shifted by a half rotor cycle. The third type switches the multiple  $\pi$ -pulses in the first type to the observed spin and a  $\pi$  or adiabatic-passage pulse to the coupled spin. All three reintroduce the same dipolar Hamiltonian under MAS but their susceptibility to non-ideal experimental conditions, especially the spinning frequency fluctuation, is drastically different. It has been shown that the first two types of REDOR pulse sequences are susceptible to small spinning frequency change but that the third type is extremely sensitive to the timing with respect to the rotor synchronization [8]. Two  $\pi$ -pulses per rotor cycle reintroduce chemical shift anisotropy (CSA) of the observed spin. The refocusing of CSA occurs at the very end of the echo sequence; therefore, it depends critically on the timing between the long evolution and refocusing periods. Small spinning frequency fluctuation, even as little as a few tenths of Hz, can accumulate the timing error over the long periods causing incomplete CSA refocusing and consequently signal fluctuation and loss

\* Fax: +1 850 644 1366.

*E-mail address:* [gan@magnet.fsu.edu](mailto:gan@magnet.fsu.edu).

[8,9]. Unfortunately, the third type pulse sequence is the only practical method for measuring distances between an observed spin-1/2 and a quadrupolar spin because typical quadrupolar frequencies are much larger than rf field strength preventing the application of multiple  $\pi$ -pulse sequence [14–18]. This contribution describes a new type of REDOR experiment that overcomes this problem for future applications with quadrupolar nuclei.

One can consider the third type pulse sequence by making the  $\pi$ -pulses longer or the spinning frequency faster. It has been shown that the finite pulse length only causes a small change on the scaling factor of the dipolar recoupling [19]. In the extreme case that the evenly spaced pulses touch each other, the multiple-pulse sequence becomes a long cw and the timing problem with rotor synchronization naturally goes away. A sequence with two touching  $\pi$ -pulses per rotor cycle implies an rf field matching the spinning frequency  $\omega_1 = \omega_r$ . That is exactly the  $n = 1$  rotary resonance condition. Rotary resonance was originally developed to recover CSA under MAS [20,21]. It has been shown that the dephasing by CSA under rotary resonance can be reversed to form a so-called rotary resonance echo [21]. Rotary resonance can also recover then refocus the heteronuclear dipolar coupling similarly to the CSA. An rf pulse to the coupled spin interrupts the refocus of heteronuclear coupling causing the rotary resonance echo to modulate. The rotary resonance echo double resonance (R-REDOR) described here measures the dipolar dephasing of rotary resonance echo for determining the heteronuclear dipolar coupling constant. It should be mentioned here that switching the  $\omega_1 = \omega_r$  rf to the coupled spin also reintroduces heteronuclear coupling known as rotary resonance recoupling ( $R^3$ ) [22,23]. However, the  $R^3$  scheme is applicable only if the coupled spin is a spin-1/2. The R-REDOR method described here is for an observed spin-1/2 coupled with a quadrupolar nucleus. Switching the  $\omega_1 = \omega_r$  rf to the observed spin-1/2 recovers both the heteronuclear dipolar coupling and the CSA though the CSA part is refocused in the form of rotary resonance echo. It will be shown that the presence of large CSA actually helps the heteronuclear recoupling by relieving the matching of the rotary resonance condition.

## 2. Rotary resonance and rotary resonance echo

Fig. 1 presents the pulse sequence and the effect of rotary resonance. The resonance occurs when an applied rf field  $\omega_1$  matches the chemical shift and dipolar coupling modulation frequencies under MAS ( $\omega_1 = n\omega_r$ ). There are mainly two resonance conditions  $n = 1, 2$  because chemical shift and dipolar coupling are second-rank tensors. These resonance conditions can be easily found by sweeping the rf field strength as shown in Fig. 1b. The  $n = 1$  resonance has a larger effect and it is used for the rest of the work. The rotary resonance phenomenon is often dominated by CSA because heteronuclear dipolar coupling is usually smaller. The resonance effect from dipolar coupling is sim-

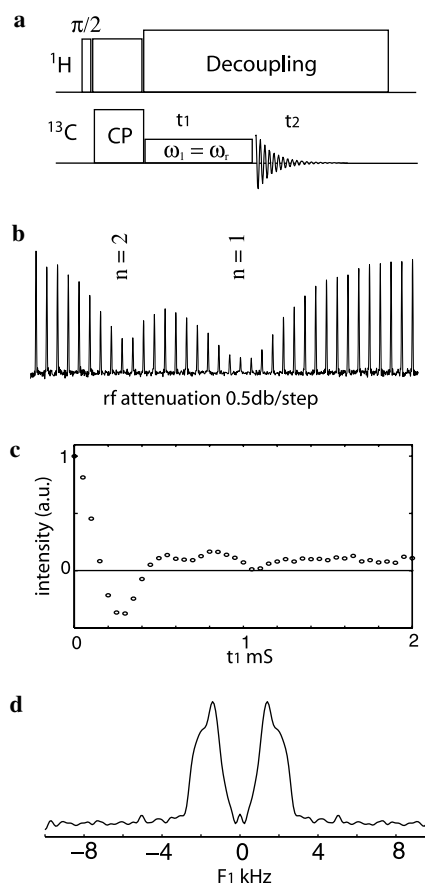


Fig. 1. (a) Rotary resonance pulse sequence, (b)  $\omega_1 = n\omega_r$  matching curve with 2 ms  $t_1$ , (c)  $n = 1$  rotary resonance time-domain signal and (d) frequency-domain spectrum. The  $^{13}\text{C}$  rf phase remains constant through the pulse sequence. The small constant component caused by rotary resonance offsets mostly due to rf field inhomogeneity in (c) is corrected before applying Fourier transformation in (d). The carbonyl carbon of natural abundant glycine was observed (14.1T magnet, 600 MHz Bruker-DRX console, 4 mm triple-resonance wide-bore MAS probe, 10 kHz spinning frequency and four scans for each measurement).

ilar to CSA as long as the spin states of the coupled nucleus remain unchanged. In this section, the rotary resonance and the echo phenomenon are demonstrated with CSA only. The dipolar coupling rotary resonance will be discussed in the following sections with the double resonance experiment.

In a frame rotating at  $n\omega_r$  about the rf field, the first-order average Hamiltonian theory can be applied to derive the resonance effect [21]. The average Hamiltonian can be described by an effective field which consists of a longitudinal component  $\omega_1 - n\omega_r$  and a transverse component  $\omega(t) = \sum_{m=-2}^2 c_m e^{-im\omega_r t}$  with respect to the rf field. The  $n = 1$  rotary resonance  $\omega_1 \approx \omega_r$  is thus driven by the first harmonic component of the chemical shift modulation  $c_1$ . The isotropic chemical shift and  $J$ -coupling are averaged to zero under the first-order approximation. For on rotary resonance, the magnetization vector rotates about an effective field perpendicular to the initial magnetization direction causing the signal to oscillate. A superposition of

oscillation frequency  $c_1$  in a powder sample yields a rapidly dephased signal (Fig. 1c) in contrary to the normal circumstance of spin-lock with  $\omega_1 \gg \omega_r$ . A Fourier transformation with respect to  $t_1$  leads to a powder line shape from which the CSA parameters can be determined. In the case of small rotary resonance offsets, the effective field becomes tilted from the transverse plane. The rotation about the tilted direction leads to a small constant component (Fig. 1c) and a zero-frequency peak in the spectrum. When the rotary resonance condition is far off ( $|\omega_1 - \omega_r| \gg c_1$ ), the constant component becomes the dominating one as a spin-lock.

The rotary resonance effect can be reversed to form an echo. There are several ways to generate rotary resonance echo. The pulse sequence in Fig. 2a shows that a half rotor cycle break (a quarter rotor cycle in the case of  $n = 2$ ) changes the phase of chemical shift modulation  $c_1$  by  $180^\circ$  [21]. The phase change reverses the direction of the magnetization vector rotation in the second half and consequently creates a rotary resonance echo. The pulse sequence in Fig. 2b uses a hard  $\pi$ -pulse. The total gap between the two rotary resonance periods including the

$\pi$ -pulse length is rotor-synchronized implying a continuing phase for the chemical shift modulation and the same direction for the effective field during the two periods. However, the spin state or the magnetization vector has been reversed or rotated by the  $\pi$ -pulse; therefore, an echo is formed in a way similar to the conventional spin-echo. The two methods are analog to the two types of rotary echo experiment, one with a sign change of the Hamiltonian by Solomon [24] and the other with a spin state inversion by Wells and Abramson [25]. It is noteworthy that a mixing of spin state inversion and sign change of Hamiltonian can cause echo destruction. Fig. 2c shows that a quarter rotor cycle change from rotor synchronization (a half rotor cycle for the total duration) results in both spin state inversion and sign change of the Hamiltonian. The combined effect makes the rotary resonance echo completely disappeared.

The decay of echo amplitude or  $T'_2$  is the most important characteristic of all echo experiments. Fig. 3 shows comparisons of  $T'_2$  decay curves of rotary resonance echo, spin-echo and multiple  $\pi$ -pulse echo (the sequence with two  $\pi$ -pulses per rotor cycle used in the third type REDOR experiment). The results show similar  $T'_2$  between the rotary resonance and the spin echo. The multiple-pulse echo is short and unstable. Two  $\pi$ -pulses per rotor cycle recover CSA and its refocusing only occurs at the very end. Gullion et al. have shown that it requires  $\pm 0.1$  Hz spinning frequency stability in order to maintain the same timing for long evolution periods for complete CSA refocusing [8,9,17]. This requirement becomes more demanding with fast spinning, large CSA and increasing magnetic fields.

The multiple  $\pi$ -pulse data in Fig. 3c was measured with the carbonyl carbon in glycine using a 600 MHz magnet. The  $10,000 \pm 2$  Hz spinning frequency stability available with the standard commercial MAS controller is not sufficient for refocusing the large CSA causing the short and fluctuating  $T'_2$  curve. Fig. 3 also shows two curves for rotary resonance and spin echo by deliberately setting the spinning frequency off by 100 Hz. The spin-echo curve becomes slightly modulated due to the large CSA and accumulated deviations from rotor-synchronization of the spin-echo sequence with long echo delay. The rotary resonance echo experiment shows no modulation but only a small change on the decay constant. The multiple-pulse echo was not even attempted for this test because of its extreme timing sensitivity. A long and stable echo is essential for measuring small dipolar coupling and the results here illustrate that the rotary resonance experiment is susceptible to spinning frequency fluctuation and rf settings for distance measurement.

### 3. Rotary resonance echo double resonance

REDOR type experiment measures the echo dephasing from heteronuclear dipolar coupling while chemical shift anisotropy and other spin interactions are completely refocused. A  $\pi$  or adiabatic pulse to the coupled spin changes

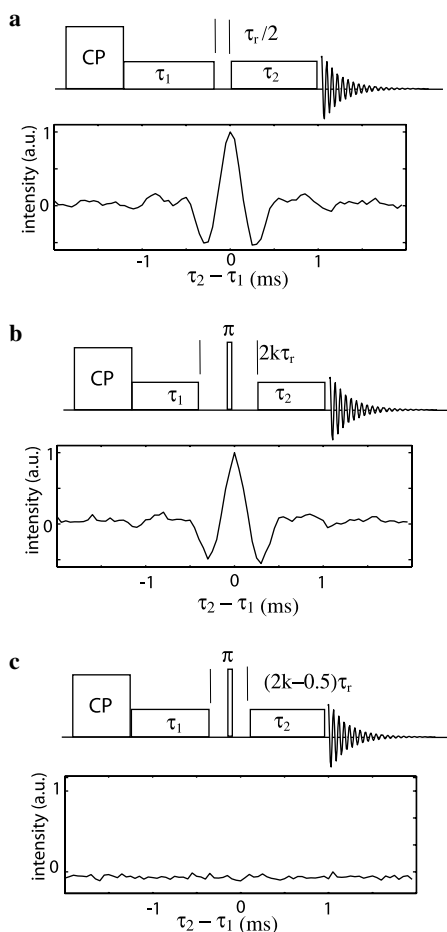


Fig. 2.  $n = 1$  rotary resonance echo by (a) a half rotor period gap and (b) by a rotor-synchronized  $\pi$ -pulse spin-echo. (c) Echo destruction by changing the total gap to  $(2k - 0.5)\tau_r$ . Experimental conditions are described in Fig. 1.

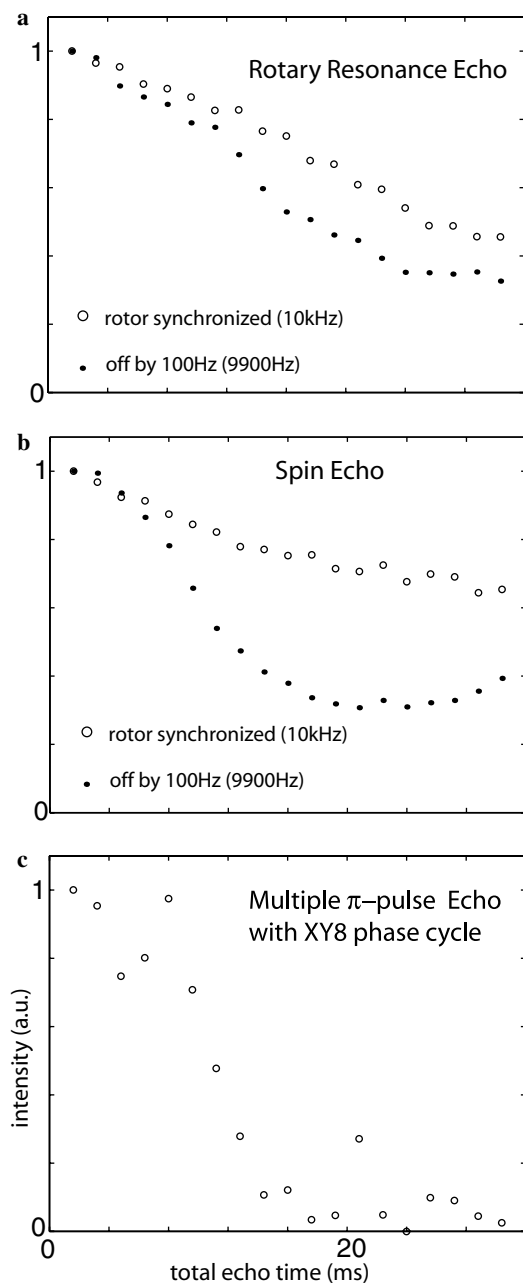


Fig. 3.  $T_2$  curves of (a) rotary resonance echo using the pulse sequence of Fig. 2b, (b) spin-echo and (c) multiple  $\pi$ -pulse (two per rotor cycle with XY-8 phase cycle [26]). The dot curves in a and b were measured with a 100 Hz MAS change from 10 to 9.9 kHz. All other experimental parameters are described in Fig. 1.

the heteronuclear dipolar coupling preventing the refocus for dipolar evolution. This section derives how heteronuclear coupling dephases rotary resonance echo in the presence of much larger chemical shift modulation and compares the result with the conventional REDOR experiment.

Under magic-angle spinning, the heteronuclear dipolar coupling consists of the first and second harmonic modulations,

$$\omega_d = 2\pi D m_S [\sin^2 \beta \cos 2(\omega_r t + \alpha) - \sqrt{2} \sin 2\beta \cos(\omega_r t + \alpha)] \quad (1)$$

Here,  $D = \gamma_I \gamma_S \hbar / 4\pi^2 r^3$  is the dipolar coupling frequency,  $\beta$  and  $\alpha$  are the polar and azimuthal angles of the internuclear vector in the rotor frame. The magnetization number  $m_S$  describes the spin states of the coupled nucleus. In the conventional REDOR with spins-1/2, the two  $\pi$ -pulses per rotor cycle change the sign of  $m_S$  twice, yielding the following average dipolar coupling [1,2]

$$\bar{\omega}_d = 4\sqrt{2} D m_S \sin(2\beta) \sin(\alpha) \quad (2)$$

The dipolar evolution continues in the echo sequence because of the two simultaneous  $\pi$ -pulses in the middle to both spins. For a spin-1/2, the two  $m_S = \pm 1/2$  spin states can be completely inverted and a powder average of the dipolar evolution  $\cos[\bar{\omega}_d \tau]$  yields the so-called universal REDOR curve [1,2].

$$S_d(\tau) = \frac{1}{4\pi} \int_0^\pi d\alpha \int_0^\pi \sin \beta d\beta \cos(\bar{\omega}_d \tau) \quad (3)$$

The dipolar evolution is a function of  $D \cdot \tau$  only and is often represented in the REDOR fraction  $1 - S_d(\tau)$ .

In rotary resonance experiment, it is the first harmonic modulation of the dipolar coupling  $d_1$  that drives the rotary resonance and echo modulation

$$d_1 = \sqrt{2} \pi D m_S \sin 2\beta \quad (4)$$

Assuming a complete absence of chemical shift anisotropy, the rotary resonance dipolar evolution is more efficient than REDOR because of the absent  $\sin(\alpha)$  in Eq. (4) as compared to the Eq. (2) ( $\int_0^\pi d\alpha \sin(\alpha) / \pi = 2/\pi$ ). However, in most practical applications, the dipolar coupling is usually measured in the presence of much larger chemical shift anisotropy. Only the dipolar frequency modulation in-phase with the chemical shift modulation then contributes to the dephasing of rotary resonance echo,

$$\omega_d^r = \sqrt{2} \pi D m_S \sin 2\beta \cos \varphi \quad (5)$$

Here, the angle  $\varphi$  is the relative phase between the dipolar and the chemical shift modulations. The chemical shift modulation does not contribute directly to the echo experiment, but it does indirectly truncate the dipolar coupling Hamiltonian. The introduction of  $\cos \varphi$  in Eq. (5) implies that only the component that commutes with the chemical shift Hamiltonian is effective for the dipolar dephasing. The results for REDOR and R-REDOR (Eqs. (2) and (5)) show the same angular dependence on  $\beta$ . Therefore, an average over  $\alpha$  and  $\varphi$  yields approximately the same dipolar dephasing curve differed only by a scaling factor  $\pi/4$  for the two experiments. This result keeps the simplicity of using the same universal REDOR curve by replacing  $\tau \rightarrow \frac{\pi}{4} \tau$ . It also makes the comparison between REDOR and R-REDOR measurements easier.

REDOR-type experiments usually perform two measurements for each evolution period, one with ( $S$ ) and the other without ( $S_0$ ) the dipolar dephasing. The dipolar coupling can be switched off by omitting the pulses to the coupled spins. The experiment without dipolar evolution  $S_0$

acts as a control that accounts for the  $T_2'$  decay and other artifacts such that the  $\Delta S/S_0 = 1 - S/S_0$  can be fitted with the universal REDOR function  $1 - S_d$  in Eq. (3). The  $1 - S_d$  curve arises from zero and tails off at one as the dimensionless parameter  $D\tau \gg 1$ .

The fitting of REDOR fraction  $\Delta S/S_0$  with  $1 - S_d$  assumes full signal participation in dipolar dephasing and complete inversion by the middle  $\pi$ -pulse to the coupled spin. In many practical applications, small portions of signal intensities do not contribute to the dipolar dephasing, for examples, due to incomplete isotope labeling and background signals. The inversion of coupled spin states may not be complete due to pulse imperfections. For the R-REDOR experiment, an additional portion comes from the rotary resonance itself. A small positive constant component is always observed in rotary resonance evolution (Fig. 1c). This component mostly comes from the rotary resonance offsets due to inhomogeneous rf field. This signal component should be accounted for the fitting of the REDOR fraction,  $\Delta S/S_0 = (1 - x)(1 - S_d)$ . Here,  $x$  is the sum of all the factors mentioned here. REDOR fraction with strong dipolar couplings quickly reaches an equilibrium value  $1 - x$  and can be used for estimating  $x$ .

More complications arise when measuring dipolar coupling with quadrupolar nuclei. First, the change of spin states of  $S > 1/2$  cannot be simply described just by a sign change of  $m_S$  (an assumption used in the derivation of the REDOR curve). Second, large modulating quadrupolar frequencies make the spin dynamics of a  $S > 1/2$  under finite rf field non-trivial. For large quadrupolar couplings, a pulse lasting  $\tau_r/3$  is often more efficient than a short  $\pi$ -pulse to scramble the spin states through adiabatic level crossings under MAS (REAPDOR) [14–18]. These issues associated with quadrupolar nuclei and REAPDOR have been addressed in a recent review article by Gullion and Vega [14] and will not be discussed further here. For the sake of avoiding these complicated issues, a spin-1/2 model compound is used here for the demonstration of the R-REDOR experiment. However, one should keep in mind that the main advantage of R-REDOR is still for measuring dipolar coupling with quadrupolar nuclei.

#### 4. Results and discussions

The R-REDOR and REDOR experiments are demonstrated using L-tryptophan with 98%  $^{15}\text{N}$ -enriched at the indole nitrogen site. The molecule has eight carbons on the aromatic and indole rings with one, two, three and four bonds from the labeled site. Dilute  $^{13}\text{C}$  spins at  $\sim 1\%$  natural abundance allow simultaneous measurements of all carbon sites without complications from  $^{13}\text{C}$  homonuclear coupling. The eight carbons are within  $\pm 15$  ppm chemical shift range that can be covered with a single rotary resonance experiment by placing the  $\nu_1 \approx 10$  kHz rf in the middle (124 ppm) of the spectrum

The R-REDOR experiment is designed primary for measuring dipolar coupling with quadrupolar nuclei; there-

fore, it should be compared with the third-type REDOR sequence (two  $\pi$ -pulses per rotor cycle applied to the observed  $^{13}\text{C}$  spin). Unfortunately, the  $\pm 2$  Hz spinning frequency control available on the commercial spectrometer cannot maintain the multiple-pulse echo long enough for the REDOR measurement (see Fig. 3c). The more robust first-type REDOR sequence (two  $\pi$ -pulses per rotor cycle applied to the coupled  $^{15}\text{N}$  spin) is used instead for the comparison. The first and the third type REDOR sequences have the same dipolar Hamiltonian; therefore, a similar REDOR curve is expected.

Fig. 4 shows the results of  $^{13}\text{C}/^{15}\text{N}$  R-REDOR and REDOR with L-tryptophan along with simulations of the fraction curves. Dipolar oscillations are evident for  $^{13}\text{C}/^{15}\text{N}$  pairs with one-bond distance and slow dephasing curves are observed for carbons with longer distances. As expected, the two experiments show similar dephasing curves with a slightly slower rate ( $\pi/4$ ) for R-REDOR. Careful comparison for the curves with short distances reveals that the R-REDOR intensities flat out at some constant levels whereas the REDOR intensities dipphase almost to zero. This constant component is a feature of rotary resonance explained in the previous section. This component comes mostly from inhomogeneous rf field and can be taken into account by the  $x$  factor in the fitting of REDOR fraction  $\Delta S/S_0 = (1 - x)(1 - S_d)$ .

REDOR fractions  $\Delta S/S_0$  of both experiments are compared with the universal REDOR curves multiplied by  $1 - x$  factor. For the REDOR experiment, the 98%  $^{15}\text{N}$ -enrichment and the  $^{15}\text{N}$   $\pi$ -pulse imperfection account only a small correction ( $x \sim 5\%$ ). For the R-REDOR experiment, an additional 17% is estimated from fitting the two curves with one-bond distance (a, h). A total of  $x \sim 22\%$  was then applied for all other carbon sites in the R-REDOR simulations. The simulations using the same dipolar coupling frequencies obtained from fitting the REDOR data are in good agreements with the rotary resonance results. The carbon sites with three-bond distance or longer (d, e and f) have dephasing curves slightly faster than the simulations. The reason for this difference is still not completely clear. It may come from different multiple-spin behaviors between the two experiments. For these sites, intermolecular  $^{13}\text{C}/^{15}\text{N}$  dipolar couplings are comparable with the intramolecular dipolar coupling. Dipolar couplings to multiple  $^{15}\text{N}$  spins may be treated differently with an isolated spin pair.

Chemical shift anisotropy plays drastically different roles between R-REDOR and REDOR experiments. The REDOR experiment is subject to the timing error for CSA refocusing, the frequency offset and finite pulse length relative to shorter rotor cycle with fast MAS. Small chemical shift anisotropy and slow spinning frequencies are preferred for REDOR applications. In contrary, the rotary resonance experiment takes advantages of the large CSA modulations and fast MAS. Indeed, it would become practically difficult, if possible, to meet the rotary resonance condition within the small dipolar couplings assuming no

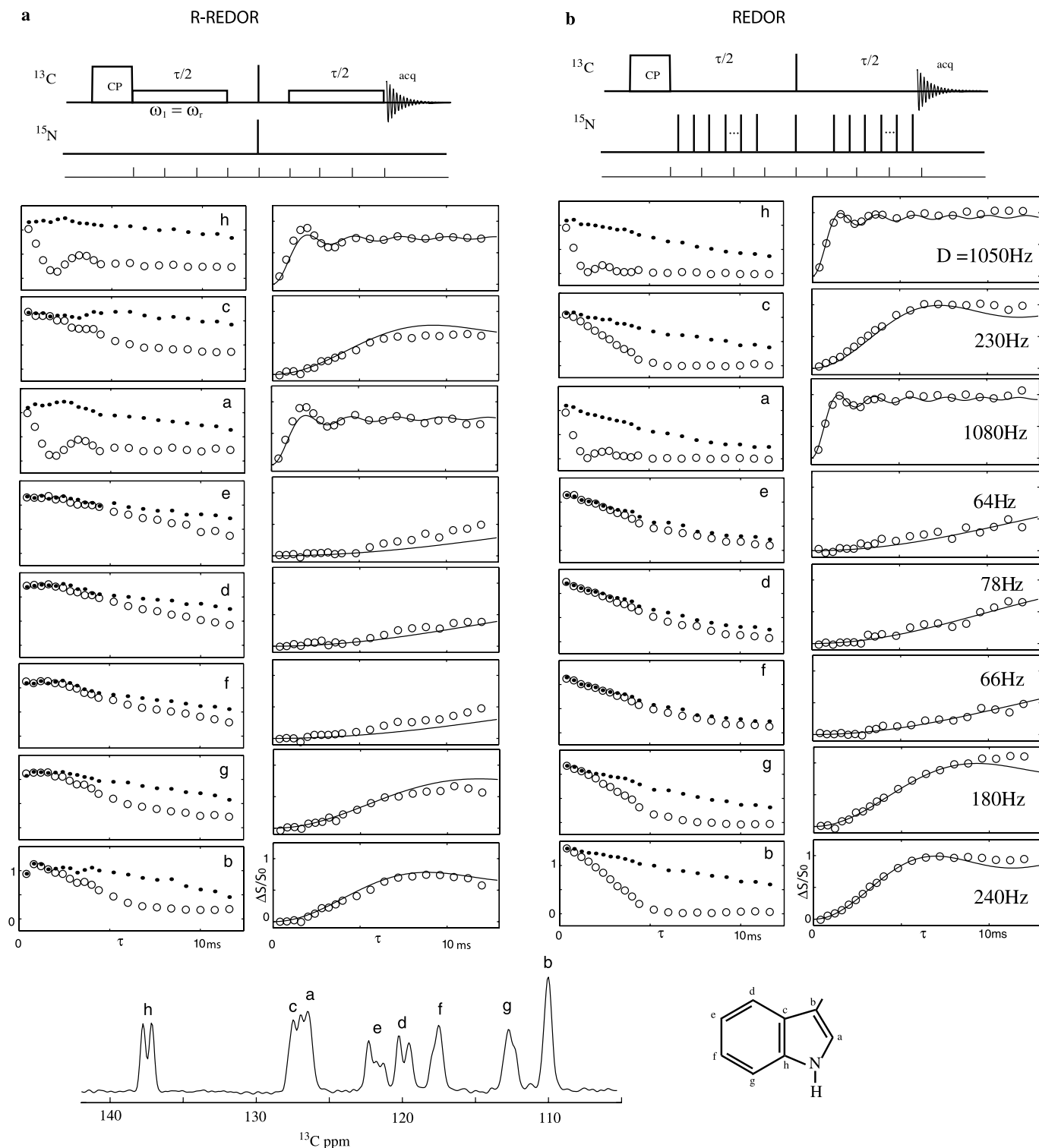


Fig. 4. (a) R-REDOR and (b) REDOR pulse sequences, experimental results and simulations of L-tryptophan with 98%  $^{15}\text{N}$ -enriched at the indole nitrogen site. In both pulse sequences, a rotor-synchronized spin-echo segment is inserted in the middle. The left column shows peak intensities with  $^{15}\text{N}$  pulses on (cycle) and off (dot). The right column shows REDOR fraction  $\Delta S/S_0$  (cycles) and simulations (solid lines). Five hundred and twelve scans with 4 s recycle delay were acquired for each spectrum. Other experimental conditions are described in Fig. 1. The MAS spectrum shows the aromatic region and peak assignments of L-tryptophan. The multiple peaks for the carbons are from non-equivalent molecules in a unit cell.

CSA. Large chemical shift modulations relieve the rotary resonance matching condition from typical 100 Hz or less of dipolar coupling to several kilohertz or more of CSA. The recoupling of small dipolar interactions can be consid-

ered as superposed on the rotary resonance of much larger CSA. In this sense, the R-REDOR experiment complements with the conventional REDOR experiment for fast spinning, large CSA and high magnetic fields.

The main advantage of R-REDOR is still for measuring dipolar coupling with quadrupolar nuclei. In this case, the third-type REDOR pulse sequence has such a strict requirement on MAS control that is not yet available with most commercial spectrometers. The rotary resonance method applies cw rf to the observed spin-1/2 for measuring dipolar couplings with quadrupolar nuclei without the limitation of extreme stable MAS control.

## 5. Conclusions

It has been shown that the rotary resonance REDOR experiment is a robust method for measuring heteronuclear dipolar recoupling. The R-REDOR method compliments with the conventional REDOR in cases of fast spinning, large CSA and high magnetic fields. The rotary resonance has a long and stable  $T_2'$  and is insensitive to spinning frequency fluctuation. The most important feature of R-REDOR is that the dipolar recoupling sequence is applied only to the observed spin; therefore, the method is applicable for measuring dipolar coupling with quadrupolar nuclei. The development of R-REDOR was initiated by recent works on indirect detected  $^{14}\text{N}$  NMR through  $^{13}\text{C}$  under MAS [27,28]. Dipolar recoupling allows the use of large dipolar coupling directly over the small  $J$  and residual dipolar–quadrupolar couplings for establishing  $^{13}\text{C}/^{14}\text{N}$  correlations and distance measurements. Rotary resonance avoids the use of any rf for dipolar recoupling to  $^{14}\text{N}$  which has very large quadrupolar couplings. The applications of rotary resonance in these areas will be published separately.

## Acknowledgments

This work is supported by the National High Magnetic Field Laboratory through National Science Foundation Cooperative Agreement DMR0084173 and by the State of Florida.

## References

- [1] T. Gullion, J. Schaefer, Rotational-echo double-resonance NMR, *J. Magn. Reson.* 81 (1989) 196–200.
- [2] T. Gullion, J. Schaefer, in: W.S. Warren (Ed.), *Advances in magnetic resonance*, vol. 13, Academic Press, New York, 1989, pp. 57–83.
- [3] S.M. Holl, G.R. Marshall, D.D. Beusen, K. Kocielek, A.S. Redlinski, M.T. Leplawy, R.A. McKay, S. Vega, J. Schaefer, Determination of an 8-angstrom interatomic distance in a helical peptide by solid-state NMR spectroscopy, *J. Am. Chem. Soc.* 114 (1992) 4830–4833.
- [4] C.A. Fyfe, K.T. Mueller, H. Grondey, K.C. Wongmoon, Dipolar dephasing between quadrupolar and spin-1/2 nuclei—REDOR and TEDOR NMR experiments on VPI-5, *Chem. Phys. Lett.* 199 (1992) 198–204.
- [5] S.O. Smith, O.B. Peersen, Solid-state NMR approaches for studying membrane-protein structure, *Annu. Rev. Biophys. Biomol.* 21 (1992) 25–47.
- [6] J.J. Balbach, J. Yang, D.P. Weliky, P.J. Steinbach, V. Tugarinov, J. Anglister, R. Tycko, Probing hydrogen bonds in the antibody-bound HIV-1 gp120 V3 loop by solid state NMR REDOR measurements, *J. Biomol. NMR* 16 (2000) 313–327.
- [7] L. Cegelski, S.J. Kim, A.W. Hing, D.R. Studelska, R.D. O'Connor, A.K. Mehta, J. Schaefer, Rotational-echo double resonance characterization of the effects of vancomycin on cell wall synthesis in *Staphylococcus aureus*, *Biochemistry* 41 (2002) 13053–13058.
- [8] J.R. Garbow, T. Gullion, The importance of precise timing in pulsed, rotor-synchronous MAS NMR, *Chem. Phys. Lett.* 192 (1992) 71–76.
- [9] E. Hughes, T. Gullion, A simple, inexpensive, and precise magic angle spinning speed controller, *Solid State Nucl. Magn. Reson.* 26 (2004) 16–21.
- [10] R.Q. Fu, S.A. Smith, G. Bodenhausen, Recoupling of heteronuclear dipolar interactions in solid state magic-angle spinning NMR by simultaneous frequency and amplitude modulation, *Chem. Phys. Lett.* 272 (1997) 361–369.
- [11] T. Gullion, C.H. Pennington, theta-REDOR: an MAS NMR method to simplify multiple coupled heteronuclear spin systems, *Chem. Phys. Lett.* 290 (1998) 88–93.
- [12] J.C.C. Chan, H. Eckert, C-rotational echo double resonance: heteronuclear dipolar recoupling with homonuclear dipolar decoupling, *J. Chem. Phys.* 115 (2001) 6095–6105.
- [13] K. Schmidt-Rohr, M. Hong, Measurements of carbon to amide-proton distances by C–H dipolar recoupling with N-15 NMR detection, *J. Am. Chem. Soc.* 125 (2003) 5648–5649.
- [14] T. Gullion, A.J. Vega, Measuring heteronuclear dipolar couplings for  $I = 1/2$ ,  $S > 1/2$  spin pairs by REDOR and REAPDOR NMR, *Prog. Nucl. Magn. Reson. Spec.* 47 (2005) 123–136.
- [15] T. Gullion, Measurement of dipolar interactions between spin-1/2 and quadrupolar nuclei by rotational-echo, adiabatic-passage, double-resonance NMR, *Chem. Phys. Lett.* 246 (1995) 325–330.
- [16] L. Chopin, S. Vega, T. Gullion, A MAS NMR method for measuring C13–O17 distances, *J. Am. Chem. Soc.* 120 (1998) 4406–4409.
- [17] E. Hughes, T. Gullion, A. Goldbourt, S. Vega, A.J. Vega, Internuclear distance determination of  $S = 1$ ,  $I = 1/2$  spin pairs using REAPDOR NMR, *J. Magn. Reson.* 156 (2002) 230–241.
- [18] Y. Ba, H.M. Kao, G.P. Grey, L. Chopin, T. Gullion, Optimizing the C13-N14 REAPDOR NMR experiment: a theoretical and experimental study, *J. Magn. Reson.* 133 (1998) 104–114.
- [19] C.P. Jaroniec, B.A. Tounge, C.M. Rienstra, J. Herzfeld, R.G. Griffin, Recoupling of heteronuclear dipolar interactions with rotational-echo double-resonance at high magic-angle spinning frequencies, *J. Magn. Reson.* 146 (2000) 132–139.
- [20] Z.H. Gan, D.M. Grant, Rotational resonance in a spin-lock field for solid-state NMR, *Chem. Phys. Lett.* 168 (1990) 304–308.
- [21] Z.H. Gan, D.M. Grant, R.R. Ernst, NMR chemical shift anisotropy measurements by RF driven rotary resonance, *Chem. Phys. Lett.* 254 (1996) 349–357.
- [22] T.G. Oas, R.G. Griffin, M.H. Levitt, Rotary resonance recoupling of dipolar interactions in solid-state nuclear magnetic-resonance spectroscopy, *J. Chem. Phys.* 89 (1988) 692–695.
- [23] M.H. Levitt, T.G. Oas, R.G. Griffin, Rotary resonance recoupling in heteronuclear spin pair systems, *Isr. J. Chem.* 28 (1988) 271–282.
- [24] I. Solomon, Rotary spin echo, *Phys. Rev. Lett.* 2 (1959) 301–302.
- [25] E.J. Wells, K.H. Abramson, *J. Magn. Reson.* 1 (1969) 378.
- [26] T. Gullion, D.B. Baker, M.S. Conradi, New, compensated Carr-Purcell sequences, *J. Magn. Reson.* 89 (1990) 479–484.
- [27] Z. Gan, Measuring amide nitrogen quadrupolar coupling by high-resolution  $^{14}\text{N}/^{13}\text{C}$  NMR correlation under magic-angle spinning, *J. Am. Chem. Soc.* 128 (2006) 6040–6041.
- [28] S. Cavadini, A. Lupulescu, S. Antonijevic, G. Bodenhausen, Nitrogen-14 NMR spectroscopy using residual dipolar splittings in solids, *J. Am. Chem. Soc.* 128 (2006) 7706–7707.